Bioorganic Chemistry 99 (2020) 103793

Contents lists available at ScienceDirect

Bioorganic Chemistry

journal homepage: www.elsevier.com/locate/bioorg

Synthesis and cytotoxic activities of organometallic Ru(II) diamine complexes

Serdar Batıkan Kavukcu[a], Onur Şahin[b], Hafize Seda Vatansever[c,f], Feyzan Ozdal Kurt[d], Mehmet Korkmaz[e], Remziye Kendirci[c], Levent Pelit[a], Hayati Türkmen[a,*]

[a] University of Ege, Faculty of Science, Department of Chemistry, 35100 Izmir, Turkey
[b] University of Sinop, Scientific and Technological Research Application and Research Center, Sinop, Turkey
[c] University of Manisa Celal Bayar, Faculty of Medicine, Department of Histology-Embryology, 45030 Manisa, Turkey
[d] University of Manisa Celal Bayar, Faculty of Sciences and Letters, Department of Biology, 45030 Manisa, Turkey
[e] University of Manisa Celal Bayar, Faculty of Medicine, Department of Medical Biology, 45030 Manisa, Turkey
[f] Research Centre of Experimental Health Sciences (DESAM), Near East University, Mersin-10, Cyprus

ARTICLE INFO

Keywords:
Ruthenium(II) arene complex
Cancer
Cytotoxicity
Bimetallic complex

ABSTRACT

A series of mono and bimetallic ruthenium(II) arene complexes bearing diamine (**Ru$_{1-6}$**) were prepared and fully characterized by ^{1}H, ^{13}C, ^{19}F, and ^{31}P NMR spectroscopy and elemental analysis. The crystal structure of the bimetallic complex (**Ru$_5$**) was determined by X-ray crystallography. Monometallic analogues (**Ru$_{1-3}$**) were synthesized to investigate the contributions of ruthenium and the other organic groups (aren, ethylenediamine, butyl) to the activity. The electrochemical behaviors of mono and bimetallic complexes were obtained from the relationship between cyclic voltammetry (CV) and the biological activities of the compounds. The cytotoxic activities of the complexes (**Ru$_{1-6}$**) were tested against wide-scale cancer cell lines, namely HeLa, MDA-MB-231, DU-145, LNCaP, Hep-G2, Saos-2, PC-3, and MCF-7, and normal cell lines 3T3-L1 and Vero. Diamine Ru(II) arene complexes have unique biological characteristics and they are promising models for new anticancer drug development. MTT analysis reveals that each synthesized Ru complex showed cytotoxic activity towards the different cancer cells. In particular, three Ru complexes (**Ru$_3$**, **Ru$_5$** and **Ru$_6$**) showed less toxic effects on the cancer cells than the others. These novel Ru complexes affected both cancer and normal cell lines. As they had a toxic effect on the cells, the dosage applied should be tested before being used for *in vivo* applications. Cytotoxicity tests have shown that the bimetallic complex **Ru$_6$** was effective on all cancer cells. The effect of bimetallic enhancement on cancer cell lines, the systematic variation of the intermetallic distance and the ligand donor properties of the mono and bimetallic complexes were explored based on the cytotoxic activity. The interaction with FS-DNA and the stability/aquation of the complexes (**Ru$_3$** and **Ru$_6$**) were investigated with ^{1}H NMR spectroscopy. The binding modes between the complexes (**Ru$_3$** and **Ru$_6$**) and DNA were investigated via UV–Vis spectroscopy.

1. Introduction

After the discovery of the anticancer activity of *cis*-platin by Rosenborg in 1965 [1], some transition metal complexes, such as platinum and ruthenium, have been studied [2–8]. Carboplatin and oxaliplatin complexes have been the most widely used agents in chemotherapeutic treatment in recent years. The relationship between the structure and activity of platinum-based chemotherapeutic agents was revealed by Reedijk [9]. Because of the side effects of platinum-based agents, interest in the other metal complexes has increased. The main problems also include the toxicity and drug resistance of developed platinum complexes on the cancer cells [10–12]. There are some negative effects of *cis*-platin, such as acute kidney problems, allergic reactions, reduced immunity to infections, gastrointestinal disorders, hemorrhage, and hearing loss. For this reason, considerable efforts have been made in this field to develop alternative metal-based anticancer drugs. Ruthenium (Ru), which is the transition metal of the platinum group that is potentially less toxic than platinum [2,13], can be found in a range of oxidation states (II, III, and IV). The rate of ligand exchange of metal complexes in aqueous solutions is important for the anticancer activity. The rate of ligand exchange of ruthenium (II, III) complexes is very similar to platinum(II) complexes [14]. Ru complexes can mimic

* Corresponding author.
E-mail address: hayati.turkmen@ege.edu.tr (H. Türkmen).

https://doi.org/10.1016/j.bioorg.2020.103793
Received 5 August 2019; Received in revised form 16 March 2020; Accepted 23 March 2020
Available online 04 April 2020

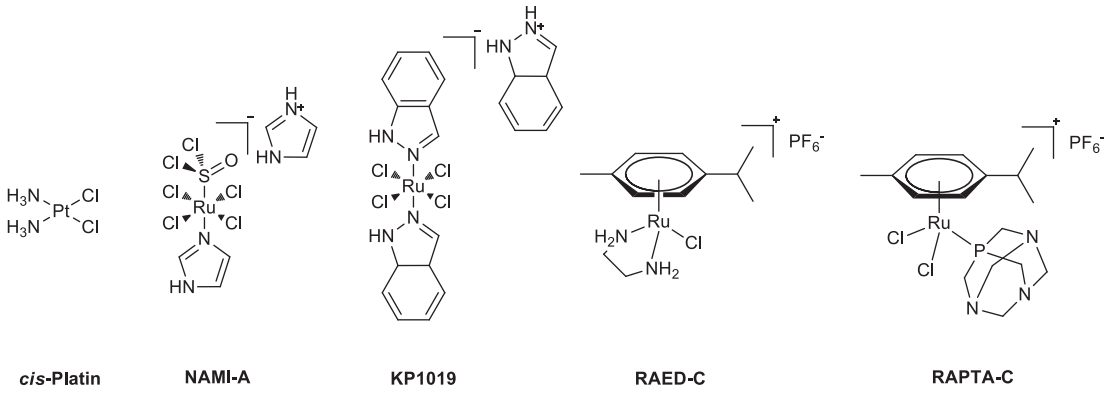

Fig. 1. *cis*-platin and ruthenium complexes used in *in vivo* treatments.

iron binding to biological molecules [15–21], such as human serum albumin and transferrin; therefore, some Ru compounds are highly selective for cancer cells. The compound $[RuCl_3(NH_3)_3]$ synthesized by Clarke was a pioneer for the anticancer activities of Ru complexes [22] and also, other Ru(III) complexes such as **NAMI-A** and **KP1019** were able to enter the *in vivo* process with low toxicity [23–26]. According to Clarke's suggestion, the activity of Ru(III) complexes was based on the reduction of Ru(II) complexes *in vivo* [27]. On the other hand, Sadler discovered the cytotoxic activity of Ru(II) arene complexes [28] and also half-sandwich Ru(II) arene complexes not only stood out as a result of their catalytic properties, but also due to their anticancer activities. Ru(II) arene complexes, which were attributed as piano stool complexes, can be classified into two main families; **RAPTA** ($[Ru(\eta^6\text{-arene})(PTA)X_6]$ (PTA: 1,3,5-triaza-7-phosphoadamantane) [11,29] and **RAED** $([Ru(\eta^6\text{-arene})(en)Cl]^+$ (en: ethylenediamine) (Fig. 1) [28,30]. These compounds include the hydrophobic arene group, a ligand containing nitrogen or phosphorus, and halogen anion. The most important property of Ru(II) arene complexes is their tunability. The arene group provides a hydrophobic surface and makes Ru stable at +2 oxidation state, which is a biologically active form. Promising results were obtained with RAED complexes against human ovarian cancer cells, especially RAED-C. This study mainly focuses on the development of RAED compounds for the treatment of common cancer tumors.

The interplay of coordination geometry, thermodynamics, and kinetic properties of the metal ions and the structural features of the ligands form a mononuclear or a set of well-defined polynuclear structures. To gain an insight into the effect of the basic nitrogen atom on the diamine ligand, the number of aryl subunits on the central phenyl scaffold and the number of metal atoms on cytotoxic activity, we synthesized a series of mono and bimetallic Ru(II) arene complexes (**$Ru_{2\text{-}6}$**) and characterized by ^1H, ^{13}C, ^{19}F and ^{31}P NMR spectroscopy and elemental analysis. Sadler et al. demonstrated that the **Ru_1** complex has promising cytotoxic activity against ovarian cancer cells [31]. In this study, we investigated the *in vitro* cytotoxic activities of mono and bimetallic complexes for different cancer cells. In addition, the **Ru_1** complex, which has notably cytotoxic activity, was used as a reference for comparison with other complexes (**$Ru_{2\text{-}6}$**). The cytotoxic activities of mono and bimetallic Ru(II) complexes were investigated in ten cell lines (HeLa, 3T3-L1, MDA-MB-231, DU-145, LNCaP, Hep-G2, Vero, Saos-2, PC-3 and MCF-7). The chemical properties and cytotoxic activities of bimetallic Ru(II) complexes were compared with monometallic analogues.

2. Results and discussions

Sadler and co-workers reported the synthesis and cytotoxic activity of Ru(II) *p*-cymene complex with *o*-phenylenediamine (*o*-pda). The *o*-pda Ru(II) complex exhibited promising cytotoxic activity against A2780 human ovarian cancer cells, with an IC50 value of 10 μM [31]. In comparison with *o*-benzoquinone diimine (*o*-bqdi) obtained by oxidation of the *o*-pda, the importance of NH proton was understood by better activity results [32]. However, the cytotoxic activity of the *o*-pda in A549 human lung cancer cells was not good. The complex **Ru_1** has been synthesized in order to investigate its cytotoxic activity in various cancer cells and to compare with our mono and bimetallic complexes due to promising results obtained in ovarian cancer cells. On the other hand, the complex $[(\eta^6\text{-}C_6H_5Ru(en)Cl]^+$ showed anticancer efficacy against A2870 cancer cells, with an IC50 value of 17 mM [28]. Recently, we have synthesized a series of mono-metallic Ru(II) complexes and investigated their catalytic properties on the alpha(α)-alkylation of ketones with alcohols [33]. These complexes included both aryl and butyl substituents. The aromatic ring on the complex provides a steric effect and hydrophobic surface, while the hydrocarbon chain group (butyl) provides solubility in oil. With these substituents, the aim was that the complexes could easily pass through the cell wall. The purpose of this study was to investigate the effects of the metal amount and ligand properties (electronic, steric and NH effect and so forth.) on cytotoxic activity (see Fig. 2).

The presence of monodentate or bidentate ligands on the complex structure is known to affect pharmacological properties [34,35]. The distance between metals on bimetallic complexes significantly affects the cytotoxic activity, and the biological activity is generally enhanced

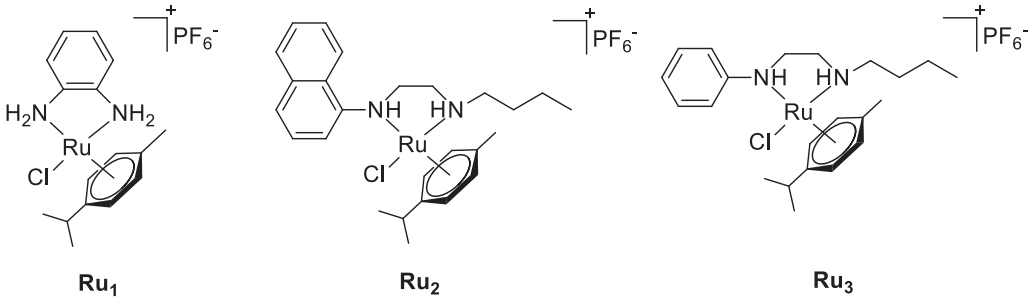

Fig. 2. Prepared complexes **$Ru_{1\text{-}3}$**.

as the amount of metal increases [36–38]. However, decreased solubility and diffusion into the cell are the main problems of the growing molecule size. Sadler and co-workers prepared long and flexible bimetallic Ru (II) arene complexes by linking two {(η^6-Bip)RuCl(en)} units with a hexamethylene chain [39]. They revealed the importance of the NH group and the bimetallic systems containing ethylenediamine. Also, four novel dinuclear ruthenium(II) arene complexes were designed by Gou et al. and they demonstrated the importance of this kind of dinuclear ruthenium(II) arene complex in drug development [40] HYPERLINK "SPS:refid::bib41" .

Aird et al. investigated the interaction of arene Ru(II) complexes with nucleic acids to gain further insight into the mechanism. In kinetic studies, they examined the reaction rate of halogen with cGMP (3′,5′-cyclic-GMP) according to different arene groups. As a result, the cytotoxic activity depends on the reaction rate, diamine NH_2 groups, the hydrophobic arene and the ancillary halogen. All played an important role in the interaction with nucleic acids [41]. The dinuclear arene Ru (II) complexes make these interactions more possible with increasing multiple ligand-binding sites [42]. Mechanism studies showed that DNA molecules were the main target of dinuclear ruthenium complexes [43]. O. Novákova et al. designed a series of dinuclear arene Ru(II) complexes with a straight-chain linker and these complexes were found to bind to DNA by forming intrastrand and interstrand crosslinks in one DNA molecule in the absence of proteins [44]. Keppler et al. investigated the effects of lipophilicity on cell toxicity with varying chain lengths [36–37]. These studies showed that dinuclear arene Ru(II) complexes have more significant biological effects than other multinuclear arene Ru(II) complexes [43]. The primary molecular target of the Ru(II) arene complexes is DNA. The Ru(II) arene complexes bind to DNA with the interaction of aromatic ligands by covalent or noncovalent interactions. These interactions induce apoptosis by causing defects in the structure of DNA [43].

2.1. Synthesis and characterization of bimetallic complexes

We synthesized the bimetallic Ru(II) complex (**Ru_4**) bridged by the 3,3-Diaminobenzidine (dab) as a analogue of the **Ru_1**. The complex **Ru_4** was obtained as a result of the reaction of [Ru(*p*-cymene)Cl_2]$_2$ with 3,3′-diaminobenzidine and NH_4PF_6 in acetonitrile. The complex **Ru_4** is an air- and moisture-stable orange solid and soluble in alcohols and DMSO (see Scheme 1).

As seen in Scheme 2, two novel bimetallic Ru(II) complexes (**$Ru_{5,6}$**) containing butyl and bridged by aryl group (1,5-naphthyl (**5**), 1,4-phenyl (**6**)) were prepared. The compounds **$A_{5,6}$** were prepared by the reaction of the aryl diamines (1,5-naphthyl (**5**), 1,4-phenyl (**6**)) with ethyl oxalyl chloride. The compounds **$B_{5,6}$** were synthesized by the reaction of compounds **$A_{5,6}$** with the *n*-butylamine. The new symmetrical pro-ligands **$C_{5,6}$** were prepared by the reduction of the compounds (**$B_{5,6}$**) with $LiAlH_4$. Finally, the new bimetallic Ru(II) complexes (**$Ru_{5,6}$**) were obtained by the reaction of ligands (**$C_{5,6}$**) with [$RuCl_2$(*p*-cymene)]$_2$ and NH_4PF_6. The bimetallic Ru(II) complexes **$Ru_{5,6}$** were highly soluble in polar solvents. They were air- and moisture-stable orange solids. The bimetallic Ru(II) complexes (**$Ru_{4\text{-}6}$**) were characterized by ^{1}H, ^{13}C, ^{19}F, and ^{31}P NMR spectroscopy, elemental analysis and cyclic voltammetry. Single crystals for the solid-state structures were obtained by the diffusion of diethyl ether into concentrated solutions of the complexes in dichloromethane. The molecular structure of the complex (**Ru_5**) was determined by single-crystal X-ray diffraction. The complex (**Ru_5**) exhibited piano-stool type geometry.

In ^{1}H NMR spectra, the *p*-cymene aromatic peaks of **Ru_5** and **Ru_6** appeared as four doublets with two protons each, while the *p*-cymene aromatic peaks of **Ru_4** were observed as two doublets with four protons each. For the bimetallic complexes **Ru_4, Ru_5** and **Ru_6**, the *p*-cymene aromatic peaks were observed at between 5.77–5.53, 5.45–3.97 and 5.61–4.71 ppm, respectively. The chemical shifts of these protons clearly indicated that the complex **Ru_4** contains the highest electron-withdrawing bridge-ligand and we can say that the electron density of the metal is less in this complex. Also, the peaks of the NH protons were observed in the range of 6.40–8.05 ppm for **Ru_4**, 6.69–6.93 ppm for **Ru_5** and 6.40–6.73 ppm for **Ru_6** (see the corresponding figures in the SI).

2.2. X-ray crystallography

The molecular structure of complex **Ru_5**, with the atom numbering scheme, is shown in Fig. 3. The asymmetric unit of complex **Ru_5** contains one Ru(II) ion, one ethylenediamine ligand, one hexafluorophosphate anion, one coordinated chlorine anion, and one *p*-cymene group. The molecule has the center of symmetry at the mid-point of the central C—C (C5—C5i) bond [(i) -x, -y + 1, -z + 1]. The bond distances of Ru-N are 2.167 (4) and 2.203 (3) Å, respectively. The Ru-Cl bond length is 2.4157 (12) Å. The molecules of **Ru_5** are connected by intermolecular N—H···F hydrogen bonds (see Table 1).

2.3. Electrochemical studies

Cyclic voltammetry (CV) results can explain the interaction of a ligand with the d orbitals of metal, and therefore reveal why the ligand is more labile to the cancer cells [46]. All complexes (**$Ru_{1\text{-}6}$**) were electroactive in the working range and showed quasi-reversible redox properties. Electrochemical oxidation/reduction couples for the same oxidation number such as $Ru^{2+/3+}$ and its reverse reaction ($Ru^{3+/2+}$) were indicated with the same index numbers in Fig. 4 (i.e. Ox1/Red1). The CV of **Ru_1** showed irreversible two-step oxidation waves with +0.59 V (Ox1) for the $Ru^{2+/3+}$ and +1.62 V (Ox2) for the $Ru^{3+/4+}$ redox reactions. In the reverse direction, a single step reduction wave with −0.78 V for the $Ru^{3+/2+}$ (Red2) was also observed. **Ru_2** complex exhibited three step oxidation/reduction waves in the working potential. The oxidation wave with −1.41 V (Ox1) in forward scan and reduction wave with −2.33 V (Red1) in reverse scan can be explained by the irreversible oxidation/reduction reaction of the ligands in the

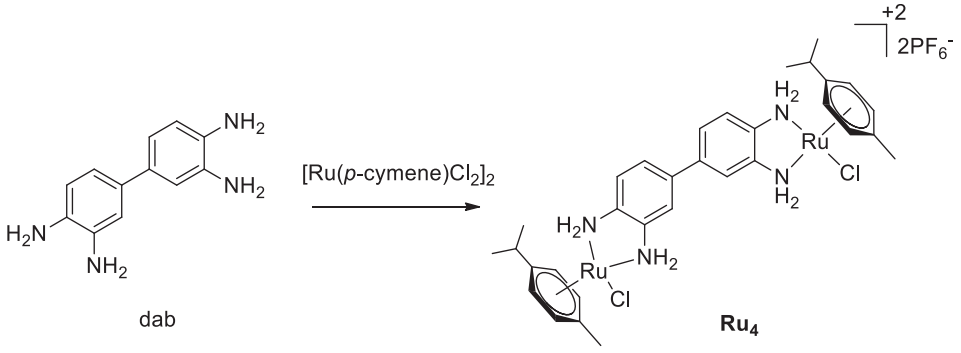

Scheme 1. Synthesis of complex **Ru_4**.

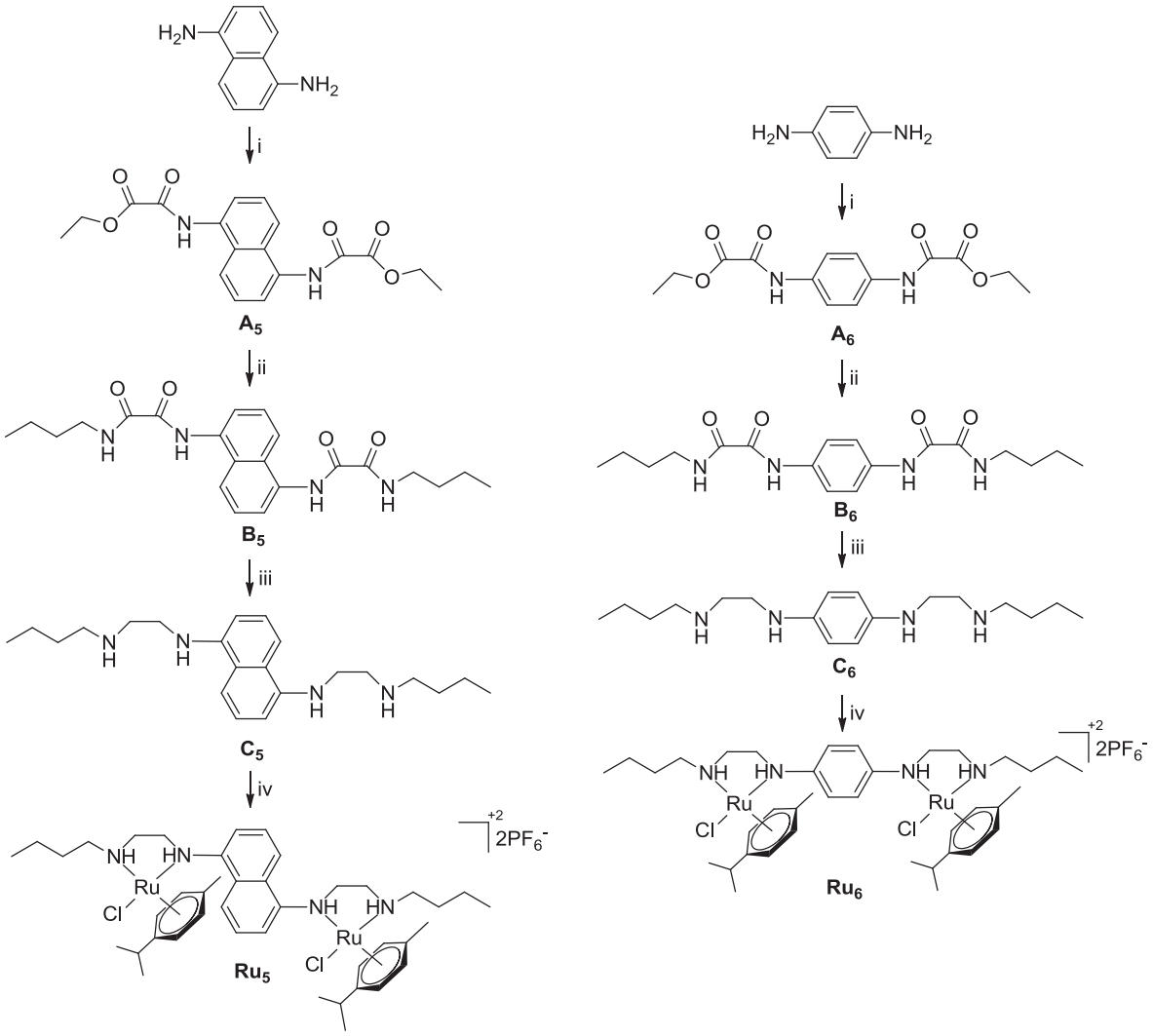

Reaction conditions: i) $C_4H_5O_3Cl$, THF, 66 °C, 1 h, ii) R-NH_2, DCM, 39 °C, 24 h, iii) $LiAlH_4$, THF, 66 °C, 48 h, iv) $[Ru(p\text{-cymene})Cl_2]_2$, MeCN, RT, 12 h.

Scheme 2. Synthesis of ligands and complexes.

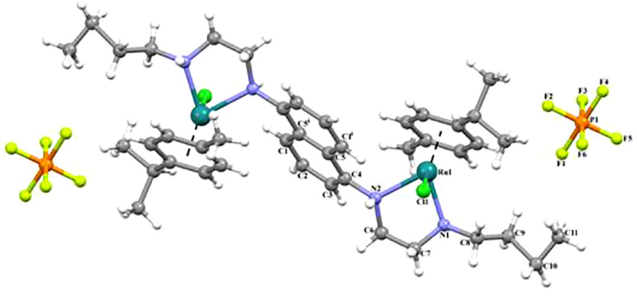

Fig. 3. Molecular structure of **Ru_5**.

complex **Ru_2** body. The oxidation wave with −0.41 V (Ox2) and reduction wave with −0.65 V (Red2) can be dedicated for the quasi-reversible redox reaction of $Ru^{2+/3+}$ redox couples. A final very high irreversible wave for $Ru^{3+/4+}$ oxidation after +1.0 V with an undefined peak potential was observed. **Ru_3** complex showed similar redox behavior to the **Ru_2** complex and the first oxidation wave with −1.45 V (Ox1) can be explained by the oxidation of the impurities in the solution. The oxidation wave with −0.20 V (Ox2) can be dedicated to the oxidation of Ru^{2+} to Ru^{3+}. A high oxidation wave was also observed after +1.0 V with undefined peak potential for $Ru^{3+/4+}$ oxidation in **Ru_3** complex. In the reverse direction, non-distinguished two step reduction waves with −0.91 V for the $Ru^{4+/3+}$ (Red 1) and −1.03 V for the $Ru^{3+/2+}$ (Red2) were observed. **Ru_4** showed different redox behavior from the others and three step irreversible oxidation and reduction waves were observed. The oxidation waves with + 0.18 V and + 1.41 V can be dedicated to two-step single-electro oxidation of Ru^{2+} to Ru^{3+} (Ox1) and Ru^{3+} to Ru^{4+} (Ox3) respectively. In the reverse direction, the reduction waves with + 0.91 V and −1.34 V can be dedicated to the reduction of Ru^{4+} to Ru^{3+} (Red3) and Ru^{3+} to Ru^{2+} (Red1) respectively. In addition, irreversible oxidation/reduction waves with + 0.57 V (Ox2) and −0.83 V (Red2) can be explained by the electrochemical reaction of different ruthenium species formed by the decomposition of unstable **Ru_4** complex. **Ru_5**

Table 1
Selected bond distance for complexes **Ru_5** (Å, °).

	Ru1-N1	Ru1-N2	Ru1-Cl1
Ru_5	2.164 (4)	2.203 (3)	2.4157 (12)

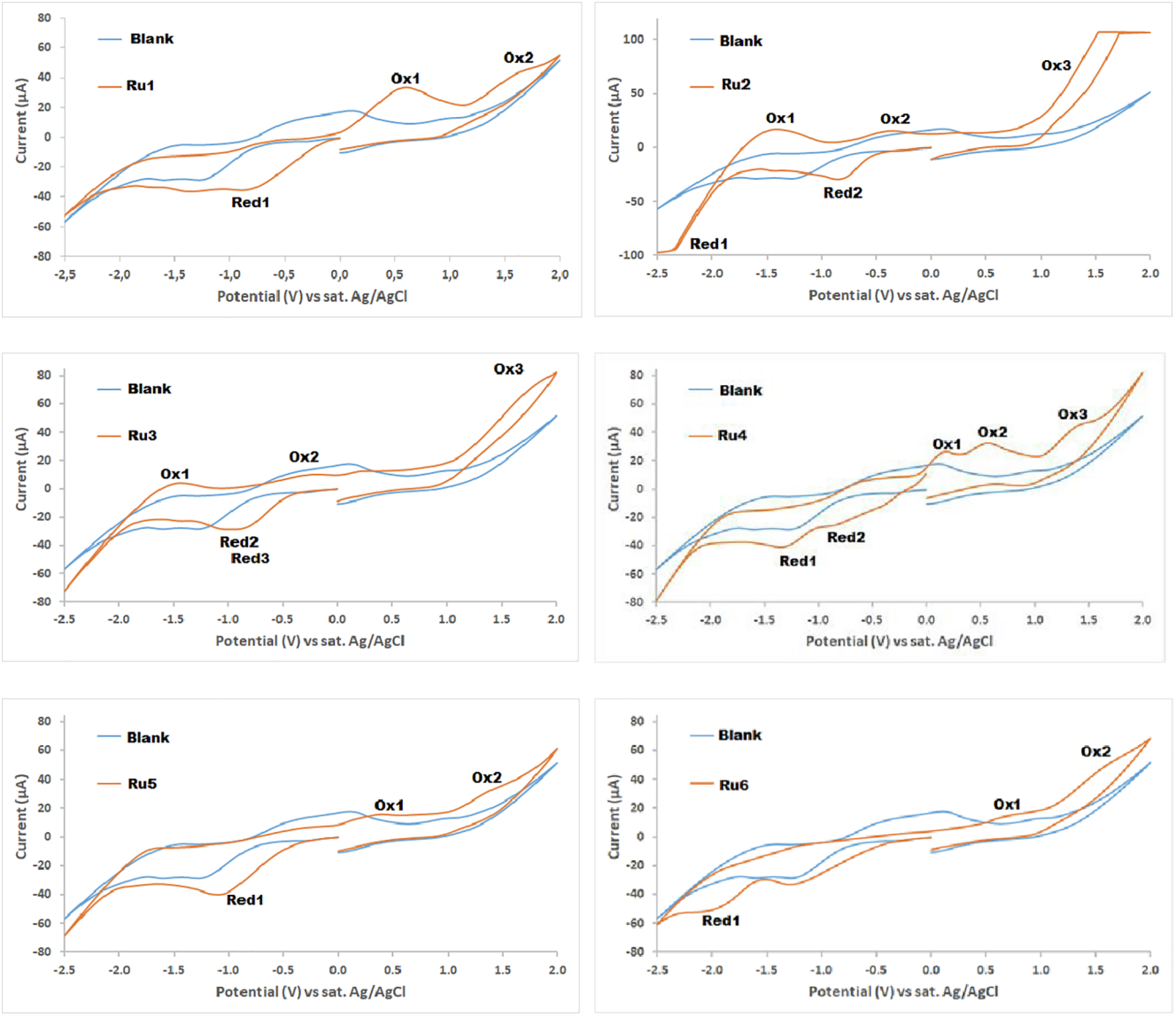

Fig. 4. Cyclic voltammogram of 5.0×10^{-4} M **Ru_1**, **Ru_2**, **Ru_3**, **Ru_4**, **Ru_5** and **Ru_6** complexes between +2.0 V and −2.5 V vs sat. Ag/AgCl.

Table 2
The redox behaviors of complexes.

Peak Potential for Redox Couples	Ru_1	Ru_2	Ru_3	Ru_4	Ru_5	Ru_6
$Ru^{2+/3+}$ Oxidation Peak (V)	+0.59	−0.41	−0.20	0.18	+0.39	+0.69
$Ru^{3+/2+}$ Reduction Peak (V)	−0.78	−0.65	−1.03	−1.34	−1.09	−1.96
$Ru^{3+/4+}$ Oxidation Peak (V)	+1.62	+1.0 <	+1.0 <	+1.41	+1.38	+1.38
$Ru^{4+/3+}$ Reduction Peak (V)	–	–	−0.91	–	–	–

complex also has similar redox behavior to **Ru_1**. Irreversible two successive oxidation waves at + 0.39 V (Ox1) and + 1.38 V (Ox2) can be dedicated to oxidation reaction of $Ru^{2+/3+}$ and $Ru^{3+/4+}$,respectively. In the reverse scan, a single step reduction wave with −1.09 V for the $Ru^{3+/2+}$ (Red2) reduction was observed. Two step irreversible oxidation waves were also observed for **Ru_6** complex. Two successive oxidation waves with + 0.69 V (Ox1) for the $Ru^{2+/3+}$ oxidation and + 1.38 V (Ox2) for the $Ru^{3+/4+}$ oxidation reactions were observed. In the reverse scan, a single step reduction wave with −1.96 V for the $Ru^{3+//2+}$ (Red2) was observed. The redox behaviors of all complexes have also been summarized in Table 2. The reduction potential of the complex is directly related to the load density of the complex. When stronger electron donor ligands are used, a smaller positive charge density will be observed in the metal ion and the reduction potential of the metal will shift to more negative potential values [44]. There is no significant difference in the reduction potential of the complex studied for Ru^{4+} to Ru^{3+} reduction. For this purpose, the Ru^{3+} to Ru^{2+} reduction potential of complexes was compared. The ease of reduction of Ru(III) to Ru(II) in the studied complexes were **Ru_2** > **Ru_1** > **Ru_3** > **Ru_5** > **Ru_4** > **Ru_6**. CV experiments showed that **Ru_2** has the smallest and **Ru_6** has the highest charge density. The highest electron density of complex **Ru_6** can be attributed to the close location of metal centers in the structure.

As previously stated, like all metal drugs, the biological activity of the ruthenium compounds is mainly related to the oxidation state of the metal center. The most biologically active form of ruthenium is

proposed as the +2 oxidation step [14]. According to the CV results, the $Ru^{2+/3+}$ oxidation potential and $Ru^{3+/2+}$ reduction potential values of the complex **Ru_6** demonstrated that the Ru (II) form of the complex is more stable (Table 2). The tendency to remain in the +2 oxidation step according to the reduction/oxidation potential of the complex **Ru_6** was reflected in the biological results, and this oxidation state also provided more biological activity.

2.4. In vitro Cytotoxicity

Cancer is a common problem because of its high prevalence and mortality rates. Therapeutic strategies for cancer treatment may lead to a reduction in the proliferation, dedifferentiation, and metastatic capability. Some treatment strategies are based on the exposure of cancer cells to toxic compounds as it triggers cell death. When new compounds are used in cancer treatment, their cytotoxic effects have to be tested. The cytotoxic activities of the complexes (**$Ru_{1\text{-}6}$**) were investigated towards HeLa, 3T3-L1, MDA-MB-231, DU-145, LNCaP, Hep-G2, Vero, Saos-2, PC-3, and MCF-7 cell lines. The potential effect of Ru complexes on cell viability was investigated by the colorimetric MTT assay. The results showed that cell proliferation and viability decreased with Ru treatment compared to control cells, although it was determined that the complexes and their effective doses were different in each cell line tested.

MTT analysis revealed that the monometallic complex **Ru_1** and the bimetallic complex **Ru_6** were more effective than the other complexes in HeLa cells and this effect was dose dependent (Fig. 5). When the concentration of the complex was increased, the cytotoxic effect of the complex on cancer cells was enhanced ($p < 0.05$). The toxic effects were observed in the 3T3-L1 cells for both **Ru_2** and **Ru_6** complexes in the MTT analysis. The numbers of cells were very low and **Ru_1**, **Ru_3**, and **Ru_4** complexes were less toxic than the other complexes, and their effects were significant in the 3T3-L1 cells ($p < 0.05$) (Fig. 6). It was found that the monometallic complex **Ru_2** was the most effective complex in DU-145 cells ($p < 0.05$). On the other hand, the bimetallic complex **Ru_6** displayed a toxic effect at all applied concentrations in DU-145 cells (Fig. 7). After statistical analysis, it was found to be significant ($p < 0.001$). All the novel Ru complexes showed a toxic effect in MDA-MB-231 cells but the most effective ones were **Ru_1**, **Ru_2** and **Ru_4** ($p < 0.05$). However, their toxicities decreased in lower dosages ($p < 0.05$) (Fig. 8). MTT analysis also revealed that **Ru_4** was the most effective agent in the androgen-dependent LNCaP cells. Interestingly, the toxicity of the complex **Ru_2** increased in a dose dependent manner ($p < 0.05$) (Fig. 9). All the novel Ru complexes showed a similar effect in Hep G2 cells, but the most effective ones were **Ru_1** and **Ru_5** ($p < 0.01$) (Fig. 10).

In Saos-2 cells, no dose-dependent effect was observed with the bimetallic complexes (**$Ru_{4\text{-}6}$**), but interestingly, the cytotoxic effect of monometallic complexes (**$Ru_{1\text{-}3}$**) increased in fewer dilutions ($p > 0.05$) (Fig. 11). In addition, the complexes **Ru_5** and **Ru_6** also showed cytotoxic effects in Vero cells.

While the effect of the bimetallic complex **Ru_5** was not significant ($p > 0.05$), the effect of the bimetallic complex **Ru_6** was significant ($p < 0.05$). However, the monometallic complexes **Ru_1** and **Ru_3** had non-toxic effects on non-cancer cells; therefore, it was concluded that they could be potential candidates as anti-cancer agents (Fig. 12).

In PC-3 cells, the cytotoxic effects of the monometallic complex **Ru_3** and the bimetallic analogue **Ru_6** were found to be more efficient than the other complexes after the MTT analysis. However, the effect of **Ru_3** was significant compared with other Ru complexes ($p < 0.05$) (Fig. 13).

While the cytotoxic effect of the bimetallic complexes **Ru_5** decreased according to its low dilutions, and the effects were detected to be significant ($p < 0.05$), the monometallic complex **Ru_2** had less effect in MCF-7 cells (Fig. 14). The efficiency difference between the complexes could be explained by the effect of bimetallic enhancement on cancer cell lines.

IC_{50} values after the MTT assay were calculated with Graphpad Prism 8 and the results are given in Table 3. According to the IC_{50} values, the monometallic complex **Ru_1** displayed a toxic effect on the control cells (3T3-L1 and Vero cells), and exhibited a moderate antiproliferative effect on HeLa, MDA-MB-231, LnCaP and MCF-7 cells. The monometallic complex **Ru_2** was considerably cytotoxic on 3T3-L1 cells, and an antiproliferative effect was observed, especially on LnCap, Hep-G2 and PC-3 cells. While the monometallic complex **Ru_3** exhibited a strong toxic effect on Vero cells, there were no antiproliferative effects on LnCap and Saos-2 cells. The bimetallic complex **Ru_4** was strongly cytotoxic on HeLa, MDA-MB-231, LnCap and MCF-7 cells. Saos-2 and PC-3 cells responded appropriately. The bimetallic complex **Ru_5** was notably cytotoxic on Vero, except Du-145, Hep-G2 and Saos-2 cells, and it had an antiproliferative effect for the rest of the cell lines. The bimetallic complex **Ru_6** showed a balanced toxic effect for the cancer cell lines. Therefore, the novel Ru complexes showed different effects on both cancer and normal cells.

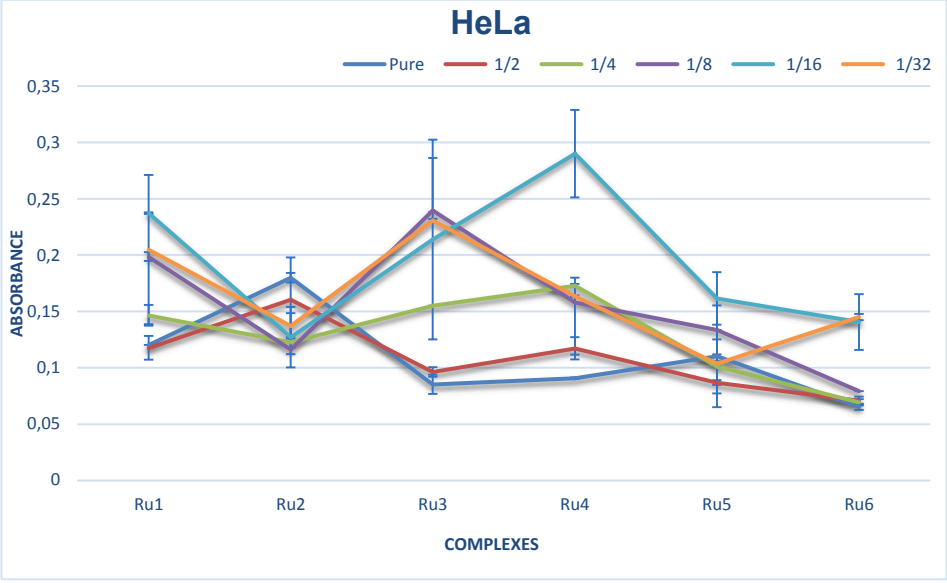

Fig. 5. MTT results of the Ru complexes effect for HeLa cells.

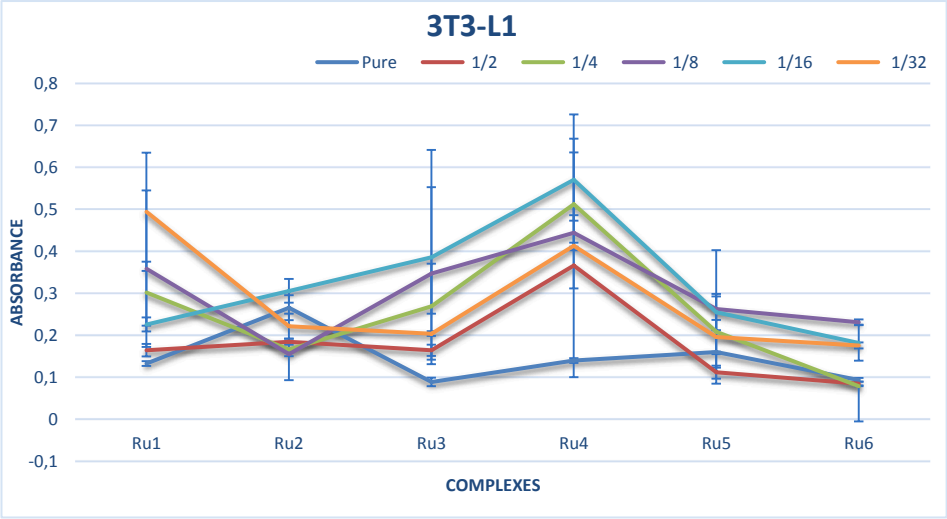

Fig. 6. MTT results of the Ru complexes effect for 3T3-L1 cells.

According to the data obtained from the MTT analysis, the novel Ru complexes showed different effects at different concentrations on the proliferation of both cancer and normal cells. All complexes had cytotoxic activity; however, high concentrations of the complexes resulted as a reduction of their effects on MCF-7 and LNCaP cells. Therefore, during *in vivo* studies, the medium concentration of Ru complexes should be considered in the treatment stage. However, the bimetallic complex **Ru$_6$** was affected in both cancer and normal cell lines. Therefore, the dosage of the complex **Ru$_6$** should be well controlled in both *in vitro* and *in vivo* studies. The high electron density on the metal center of complex **Ru$_6$** also resulted in higher cytotoxic activity.

2.5. Stability/aquation of the complexes Ru_3 and Ru_6

The stability or aquation of metal-based anticancer drugs directly affects their biological properties. To study the biological properties of metal-based anticancer drugs with low or no solubility in water, stock solutions are usually prepared in DMSO. In such cases, the chloride ion in the complex structure is exchanged by water or any solvent's molecules like DMSO. In this mechanism, the aquation step is important for the interaction with DNA base pairs or with proteins to form adducts. Thus, the time-dependent hydrolysis was monitored to reveal the aquation and stability of the monometallic complex **Ru$_3$** and the bimetallic complex **Ru$_6$** in a D_2O/DMSO-d_6 (20:80) solvent system by ^{1}H NMR spectroscopy. The complexes (**Ru$_3$** and **Ru$_6$**) were hydrolyzed quickly and the equilibrium was reached when they were just prepared. The stability of the complexes was also examined with ^{19}F- and ^{31}P NMR spectroscopies. The complexes were pure in the solution according to ^{1}H-, ^{19}F- and ^{31}P NMR spectrums for 45 days (Fig. S14 and S15 in the SI) (see Figs. 15 and 16).

2.6. Interaction of the complexes Ru_3 and Ru_6 with FS-DNA

Inorganic metal-based drugs show their therapeutic effects through coordination to DNA or proteins. This coordination can be via intra- or inter-DNA–DNA, DNA–protein, and protein–protein crosslinks. This is called a fragment-based approach and its application to metal-based drugs is becoming widespread [45]. This approach is considered to be an important way of designing bioactive compounds. The interaction of the monometallic complex **Ru$_3$** and the bimetallic complex **Ru$_6$** with FS-DNA (fish sperm-DNA) was investigated by ^{1}H NMR spectroscopy in DMSO-d_6 at ambient temperature (see the corresponding figures in the SI). The addition of an equal of FS-DNA to an equilibrated solution of **Ru$_3$** or **Ru$_6$** in DMSO-d_6 induced relatively fast changes in the ^{1}H NMR spectrums (Figure S11 and S12 in the SI). Binding of a Ru(II) center to N atom of FS-DNA moieties typically induces a downfield shift of the aromatic region resonances in the ^{1}H NMR spectrums compared to the free FS-DNA.

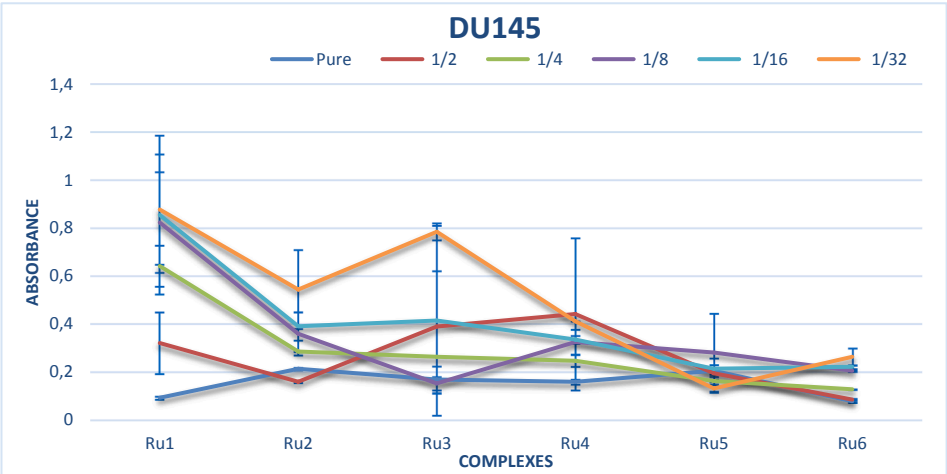

Fig. 7. MTT results of the Ru complexes effect for DU-145 cells.

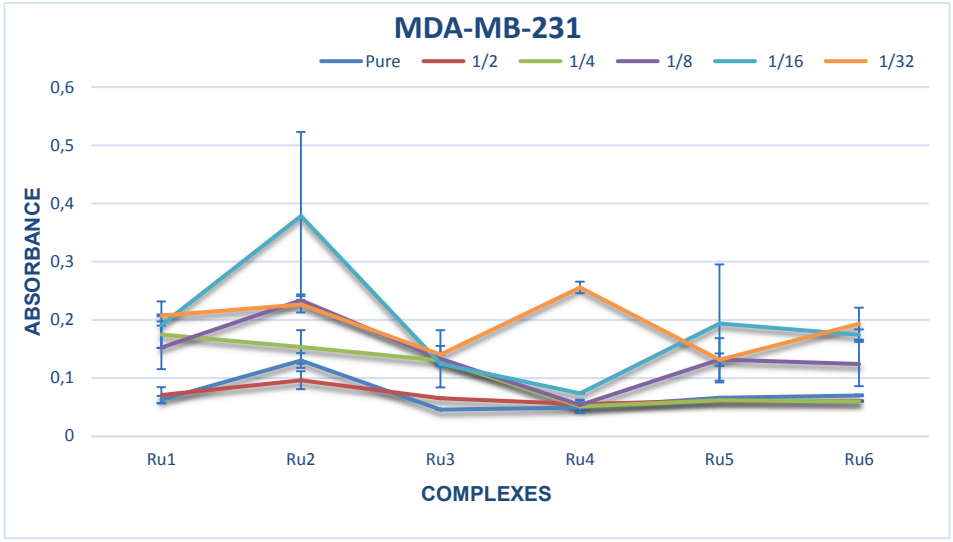

Fig. 8. MTT results of the Ru complexes effect for MDA-MB-231 cells.

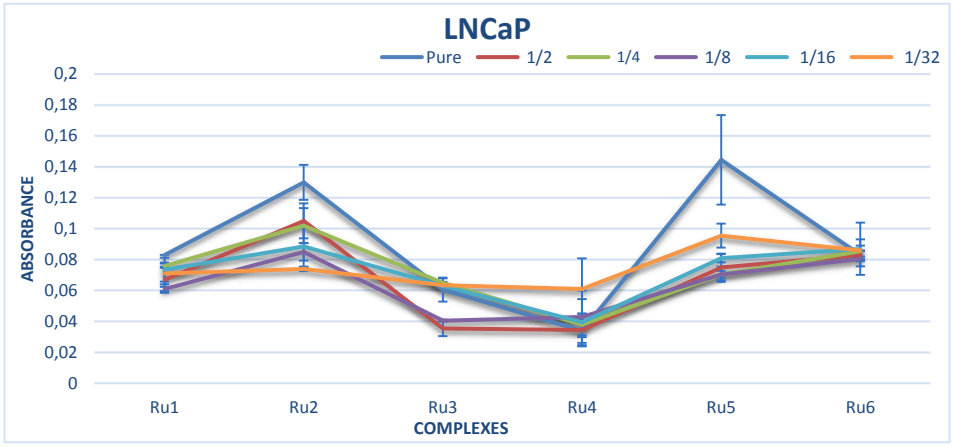

Fig. 9. MTT results of the Ru complexes effect for LNCaP cells.

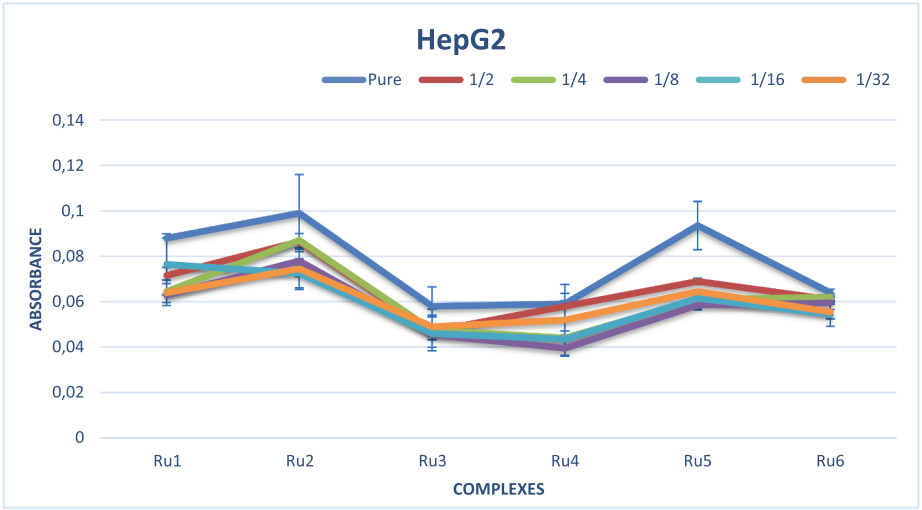

Fig. 10. MTT results of the Ru complexes effect for Hep-G2 cells.

2.7. DNA binding studies

Ru(II) arene complexes can bind to DNA through both covalent (replacement of an ancillary halogen ligand) and non-covalent (groove binding, electrostatic or intercalation) interactions [43]. Therefore, it is important to determine the DNA binding properties of Ru(II) arene complexes. The UV–Vis technique, which is an electronic absorption spectroscopy, is a good application for the investigation of the binding

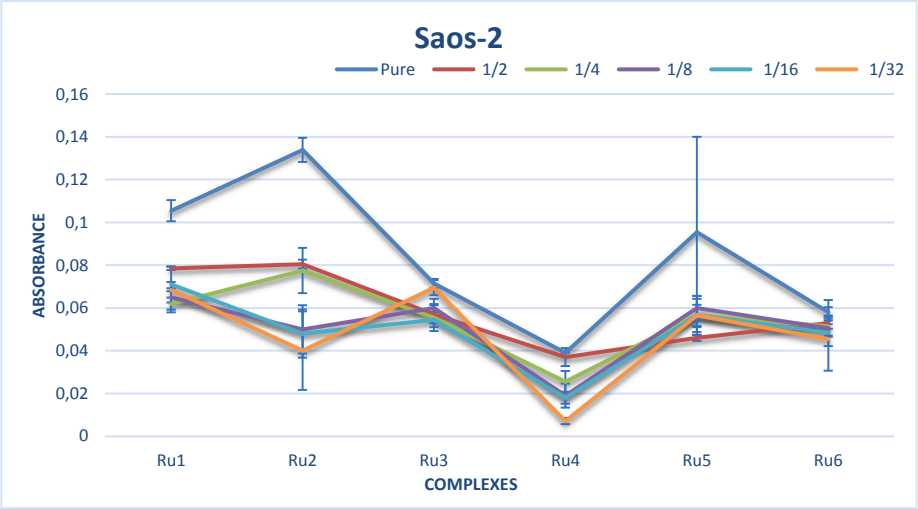

Fig. 11. MTT results of the Ru complexes effect for Saos-2 cells.

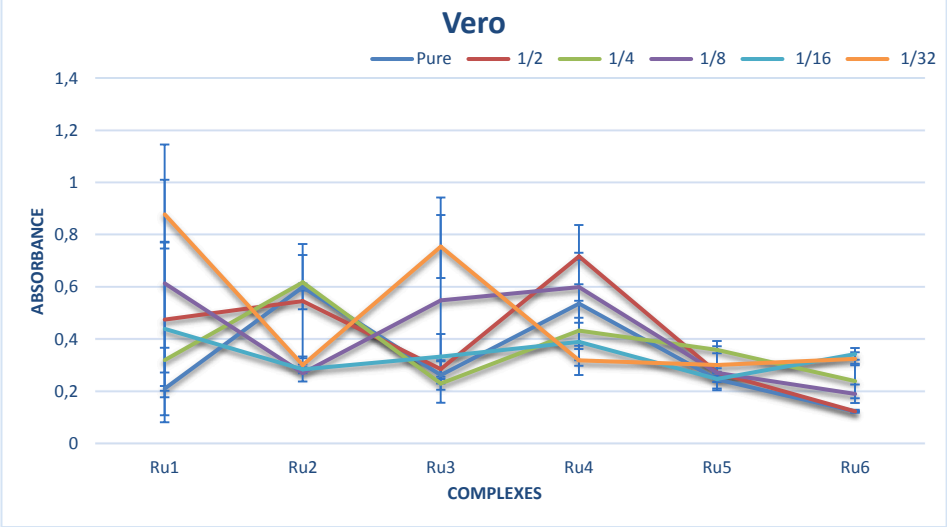

Fig. 12. MTT results of the Ru complexes effect for Vero cells.

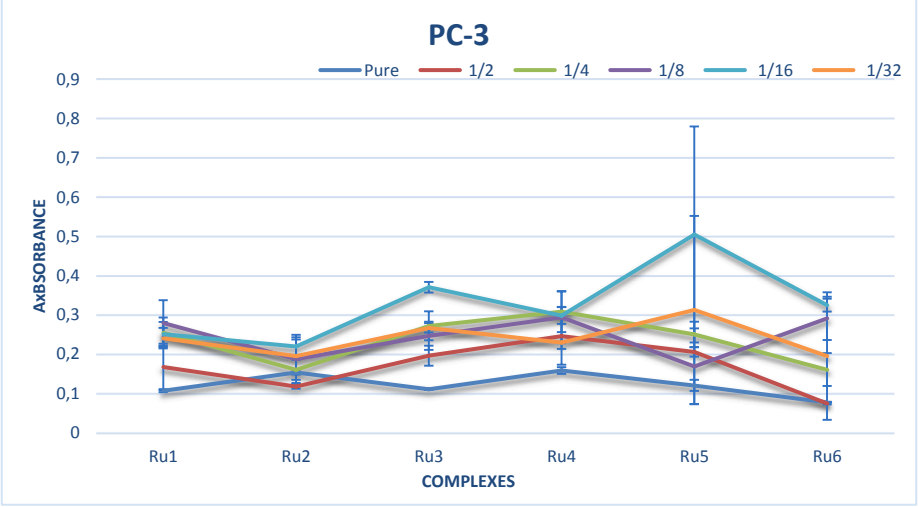

Fig. 13. MTT results of the Ru complexes effect for PC-3 cells.

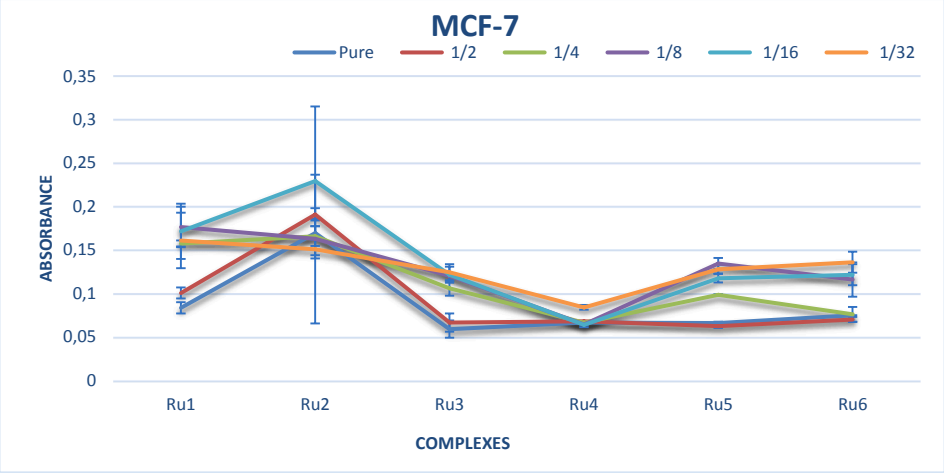

Fig. 14. MTT results of the Ru complexes effect for MCF-7 cells.

properties with DNA [50]. In order to investigate these interactions, we performed UV–Vis analyses of the complexes **Ru_3** and **Ru_6** (0–15 μM) in 20 mM Tris-HCl/NaCl (pH: 7.0) with 0.1 mM FS-DNA and the absorption spectra were given in Fig. 17. The absorption differences in hypochromic and hyperchromic values indicated non-covalent interactions between DNA and the complexes. The hyperchromism in the absorption intensity of FS-DNA at λ_{max} = 260 nm for both complexes was related with the non-covalent intercalation between DNA and the complexes. The intrinsic binding constants K_b of the complexes (**Ru_3** and **Ru_6**) were (1.7 ± 0.1) × 10^5 M^{-1} and (7.6 ± 0.1) × 10^4 M^{-1}, respectively. The K_b values suggested intense binding of the complexes to FS-DNA.

3. Conclusions

In summary, we have reported a series of mono and bimetallic Ru (II) *p*-cymene complexes carrying the diamine ligand group. These complexes were characterized by spectroscopic methods and analyzed by CV. The complex **Ru_1**, known to be cytotoxically active in the literature, was used as a reference in this study. The effects of monometallic (**$Ru_{1\text{-}3}$**) and bimetallic (**$Ru_{4\text{-}6}$**) complexes, which were analogues and had different dilution rates, on cytotoxic activity were investigated. Subtle differences in the coordination of the ligand may produce important differences in its electron donation, thus producing an important impact on the cytotoxic efficacy. Subtle ligand modifications on Ru(II) arene complexes can lead to different mechanisms of action and result in significant changes in the cytotoxic efficacy. In conclusion, after MTT analysis, new synthesized Ru complexes have different effects on different cancer cell lines depending on the dosage manner. These new synthesized Ru(II) arene complexes could have a greater trigger effect on cell death pathways with good cellular tolerance. Therefore, when performing them in *in vivo* application, proper doses need to be determined. Among the complexes, the highest cytotoxic activity and also the highest electron density on metal centers was observed in the bimetallic complex **Ru_6**. The complexes (**Ru_3** and **Ru_6**) were stable for 45 days in a D_2O/DMSO-d_6 (20:80) solvent system. The interaction of the complexes (**Ru_3** and **Ru_6**) with FS-DNA was also examined. When the reactivity of the mono and the bimetallic complexes was examined, it was observed that the introduction of a second metal fragment increased the reactivity and stability with biomolecular targets and led to an antimetastatic increase; potentially, a lower dose of the drug may be used, which could reduce side effects.

4. Experimental section

4.1. General information

Reactions involving air-sensitive components were performed by using a Schlenk-type flask under argon atmosphere and high vacuum-line techniques. The glass equipment was heated under vacuum in order to remove oxygen and moisture and then it was filled with argon. The solvents were analytical grade and distilled under argon atmosphere from sodium (tetrahydrofuran, toluene, diethylether, pentane), P_2O_5 (dichloromethane). Reagents were purchased from Aldrich or Merck and were used as received. ^{1}H-, ^{13}C-, ^{19}F- and ^{31}P NMR spectra were recorded on a Varian 400 MHz spectrometer. *J* values were given in Hz. X-Ray diffraction analysis was performed on a D8-QUEST diffractometer equipped with graphite-monochromatic Mo-Ka radiation.

Table 3
IC_{50} values of the Ru complexes after MTT assay (μM).[a]

Cells	IC_{50} (μM)					
	Ru_1	Ru_2	Ru_3	Ru_4	Ru_5	Ru_6
HeLa	16.3 ± 1.2	41.3 ± 1.6	24.2 ± 1.3	9.4 ± 0.9	8.2 ± 0.9	9.7 ± 6.2
3T3-L1	11.0 ± 1.0	2.0 ± 0.3	28.9 ± 1.4	46.5 ± 1.6	13.3 ± 0.9	17.6 ± 1.2
DU-145	34.5 ± 1.5	12.2 ± 1.0	14.6 ± 1.3	30.3 ± 1.4	55.9 ± 1.7	15.7 ± 1.1
MDA-MB-231	26.0 ± 1.4	11.2 ± 1.0	37.9 ± 1.5	5.4 ± 0.7	12.7 ± 1.1	11.8 ± 1.0
LNCaP	20.0 ± 1.3	27.6 ± 1.4	82.8 ± 1.9	5.2 ± 0.7	32.2 ± 1.6	27.5 ± 1.4
Hep-G2	54.9 ± 1.7	29.2 ± 1.4	59.6 ± 1.7	30.6 ± 1.4	55.9 ± 1.7	14.9 ± 1.1
Saos-2	55.6 ± 2.8	39.3 ± 1.5	> 100	15.6 ± 1.1	70.6 ± 1.8	22.7 ± 1.3
Vero	10.8 ± 1.0	17.6 ± 1.2	7.2 ± 0.8	20.3 ± 1.3	0.19 ± 0.2	14.7 ± 1.1
PC-3	41.8 ± 1.6	20.0 ± 1.3	21.9 ± 1.3	23.4 ± 1.2	8.8 ± 0.9	20.8 ± 1.3
MCF-7	34.7 ± 1.5	38.4 ± 1.8	31.0 ± 1.4	4.4 ± 0.6	25.0 ± 1.3	14.5 ± 1.1

[a] IC50 values are presented as mean ± SD (standard error of the mean) from three repeating experiments.

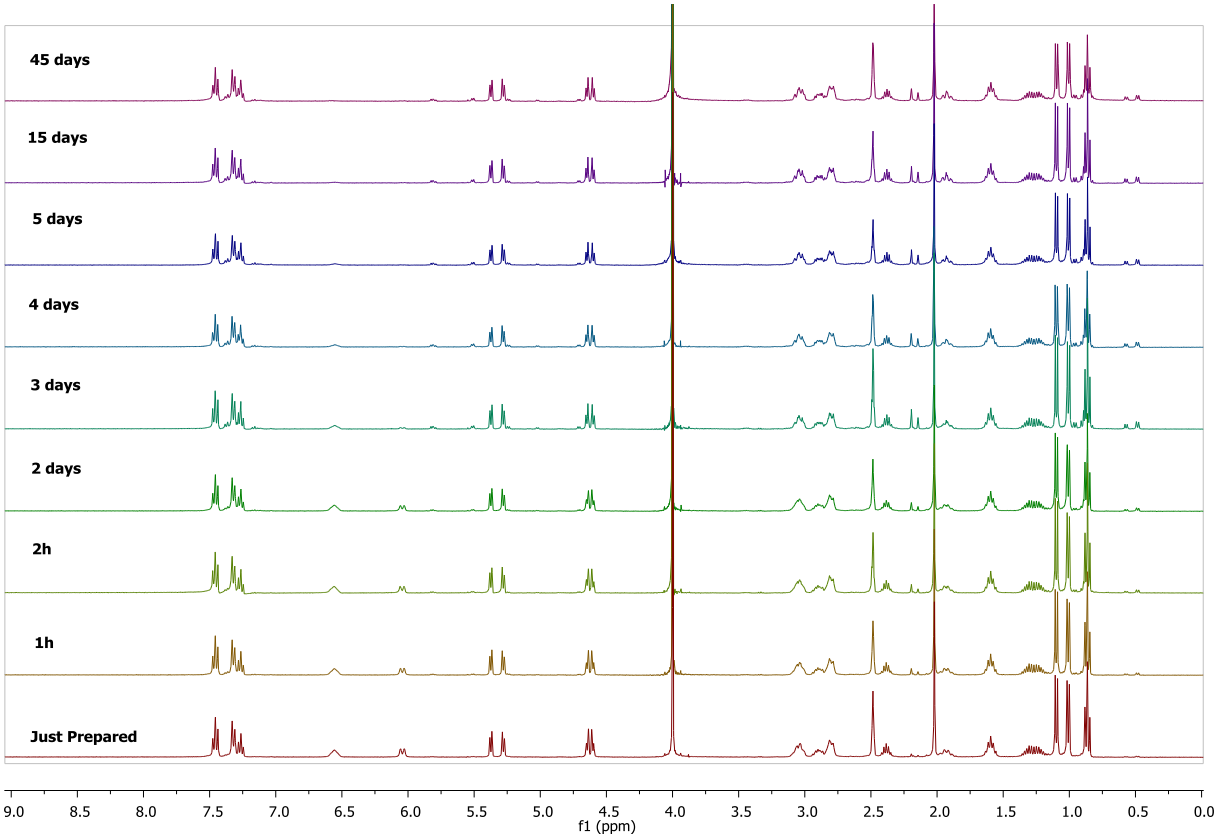

Fig. 15. The stability of $\mathbf{Ru_3}$ was monitored via ^{1}H NMR spectroscopy in 20% D_2O/DMSO-d_6 over 45 days.

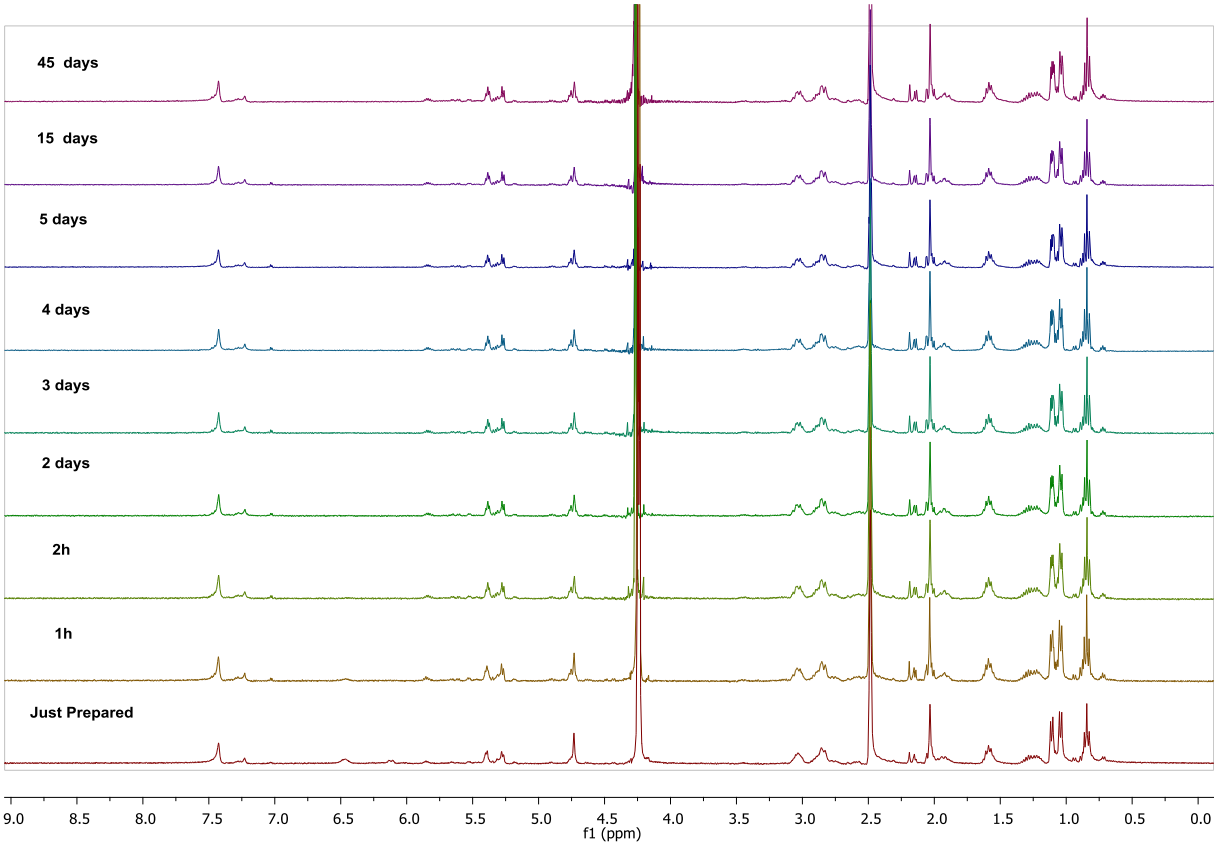

Fig. 16. The stability of $\mathbf{Ru_6}$ was monitored via ^{1}H NMR spectroscopy in 20% D_2O/DMSO-d_6 over 45 days.

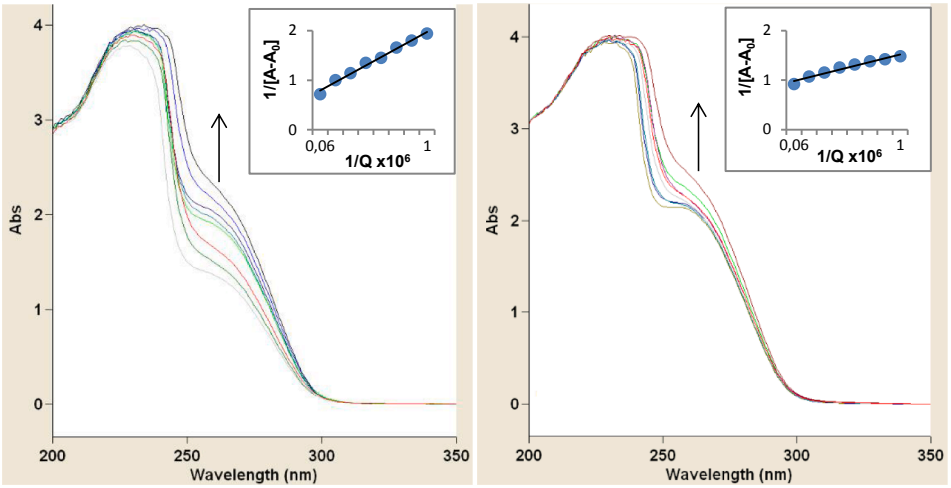

Fig. 17. Absorption spectra of FS-DNA with increasing concentrations of the complexes **Ru$_3$** (left) and **Ru$_6$** (right) (arrow shows the increase of the intensity on increasing complex concentration). K_b was calculated by the ratio of intercept and slope of plot between $1/(A_0 - A)$ and $1/[Q]$.

Melting points were measured on Gallenkamp electrothermal melting point apparatus without correction. The cyclic voltammetry (CV) studies were carried out with an Autolab 204 electrochemical system with three electrode assemblies. $RuCl_2$(*p*-cymene)]$_2$ was prepared according to the method reported by Bennett and Smith through the reaction of ruthenium(III) chloride with α–terpinene [47]. **Ru$_1$** was synthesized according to the procedure published by Sadler [31]. All synthesis procedures are available in the paper previously published by our group [33].

4.2. Synthesis and characterization of compounds A

Compound A$_5$: The compound **A$_5$** was prepared in the same manner as our published procedure using 1,5-diaminonaphthalene (1.00 g, 6.32 mmol), ethyl oxalyl chloride (2.07 mL, 18.50 mmol). Yield: 1.63 g (72%). White solid. m.p.: 215 °C. ^{1}H NMR (400 MHz, DMSO): δ 10.94 (s, 2H, N*H*), 7.94 (t, $J_{H\text{-}H}$ = 4.4 Hz, 2H, Ar-*H*), 7.60 (s, 2H, Ar-*H*), 7.59 (s, 2H, Ar-*H*), 4.37 (q, 4H, OCH_2CH$_3$), 1.36 (t, $J_{H\text{-}H}$ = 7.2 Hz, 3H, OCH$_2$CH_3). ^{13}C NMR (400 MHz, DMSO): δ 161.2, 157.4, 132.9, 129.7, 126.1, 124.3, 122.5, 62.7, 14.3.

Compound A$_6$: The compound **A$_6$** was prepared in the same manner as our published procedure using *p*-phenylenediamine (1.00 g, 9.25 mmol), ethyl oxalyl chloride (2.07 mL, 18.50 mmol). Yield: 2.17 g (76%). White solid. m.p.: 208 °C. ^{1}H NMR (400 MHz, DMSO): δ 10.70 (s, 2H, N*H*), 7.70 (s, 4H, Ar-*H*), 4.30 (m, 4H, OCH_2CH$_3$), 1.30 (t, $J_{H\text{-}H}$ = 7.2 Hz, 6H, OCH$_2$CH_3). ^{13}C NMR (400 MHz, DMSO): δ 161.1, 155.8, 134.5, 121.2, 62.8, 14.2.

4.3. Synthesis and characterization of compounds B

Compound B$_5$: The compound **B$_5$** was prepared in the same manner as our published procedure using **A$_5$** (1.00 g, 3.24 mmol) and *n*-butylamine (0.64 mL, 6.48 mmol). White solid. m.p.: 285 °C. ^{1}H NMR (400 MHz, DMSO): δ 10.55 (s, 2H, N*H*), 8.91 (t, 2H, N*H*), 7.75 (s, 4H, Ar-*H*), 3.17 (m, 4H, CH_2), 1.46 (s, 4H, CH_2), 1.26 (s, 4H, CH_2), 0.87 (t, $J_{H\text{-}H}$ = 7.6 Hz, 6H, CH_3).

Compound B$_6$: The compound **B$_6$** was prepared in the same manner as our published procedure using **A$_6$** (1.00 g, 2.79 mmol) and *n*-butylamine (0.56 mL, 5.58 mmol). Yield: 1.03 g (90%). White solid. m.p.: 274 °C. ^{1}H NMR (400 MHz, DMSO): δ 10.73 (s, 2H, N*H*), 8.93 (t, 2H, N*H*), 7.78 (d, $J_{H\text{-}H}$ = 8.0 Hz, 2H, Ar-*H*), 7.60 (m, 4H, Ar-*H*), 3.23 (m, 2H, CH_2), 1.52 (s, 4H, CH_2), 1.31 (s, 4H, CH_2), 0.91 (t, $J_{H\text{-}H}$ = 7.2 Hz, 6H, CH_3).

4.4. Synthesis and characterization of compounds C

Compound C$_5$: The compound **C$_5$** was prepared in the same manner as our published procedure using **B$_5$** (1.00 g, 2.76 mmol.) and $LiAlH_4$ (1.05 g, 27.62 mmol). Yield: 0.59 g (69%). Yellow oil. ^{1}H NMR (400 MHz, 303 K, $CDCl_3$): δ 7.25 (s, 2H, N*H*), 6.58 (s, 4H, Ar-*H*), 3.16 (m, 4H, CH_2), 2.85 (m, 4H, NCH_2CH$_2$N), 2.62 (m, 4H, NCH$_2$CH_2N), 1.48 (m, 4H, CH_2), 1.36 (m, 4H, CH_2), 0.91 (t, $J_{H\text{-}H}$ = 4.0 Hz, 6H, CH_3). ^{13}C NMR (100 MHz, 303 K, $CDCl_3$): δ 140.9, 114.9, 49.3, 48.8, 44.8, 32.0, 20.4, 13.9.

Compound C$_6$: The compound **C$_6$** was prepared in the same manner as our published procedure using **B$_6$** (1.00 g, 2.42 mmol.) and $LiAlH_4$ (0.92 g, 24.24 mmol). Yellow oil. ^{1}H NMR (400 MHz, $CDCl_3$): δ 7.32 (m, 4H, Ar-*H*), 6.62 (d, $J_{H\text{-}H}$ = 7.6 Hz, 2H, Ar-*H*), 3.35 (m, 4H, CH_2), 3.02 (m, 4H, NCH_2CH$_2$N), 2.67 (m, 4H, NCH$_2$CH_2N), 1.52 (m, 4H, CH_2), 1.41 (m, 4H, CH_2), 0.93 (t, $J_{H\text{-}H}$ = 7.2 Hz, 6H, CH_3). ^{13}C NMR (100 MHz, $CDCl_3$): δ 144.3, 125.3, 124.2, 109.0, 104.5, 49.2, 48.4, 43.6, 32.3, 20.4, 14.0.

4.5. Synthesis and characterization of Ru complexes

Complex Ru$_4$: The complex **Ru$_4$** was prepared in the same manner as our published procedure using 3,3′-Diaminobenzidine (1.00 g, 4.67 mmol), $[RuCl_2$(*p*-cymene)]$_2$ (2.86 g, 4.67 mmol) and NH_4PF_6 (1.51 g, 9.34 mmol). 3.58 g (72%). Brown powder. m.p.: 165 °C. Elemental analysis: calcd (%) for $C_{32}H_{42}Cl_2F_{12}N_4P_2Ru_2$ (MW: 1045,68): C, 36.76; H, 4.05; N, 5.36%. Found: C, 36.80; H, 4.03; N, 5.34%. ^{1}H NMR (400 MHz, DMSO): δ 8.07 (br, 2H, N*H*), 7.36 (m, 3H, Ar-*H*), 6.42 (m, 2H, N*H*), 5.76 (d, $J_{H\text{-}H}$ = 6.4 Hz, 2H, *p*-cymene-Ar-*H*), 5.54 (d, $J_{H\text{-}H}$ = 5.2 Hz, 2H, *p*-cymene-Ar-*H*), 2.89 (m, 1H, CH_2), 2.22 (s, 3H, *p*-cymene-CH_3), 1.19 (d, $J_{H\text{-}H}$ = 6.8 Hz, 6H, *p*-cymene- CH(CH_3)$_2$). ^{13}C NMR (100 MHz, DMSO): δ 141.0, 140.0, 137.6, 127.0, 125.4, 124.1, 103.1, 98.5, 82.5, 80.6, 30.5, 22.6, 18.4. ^{19}F NMR (376 MHz, DMSO): δ −69.1, −71.0 (d, $J_{F\text{-}F}$ = 711.0 Hz, PF_6). ^{31}P NMR (166 MHz, DMSO): δ −144.0 (septed, $J_{P\text{-}P}$ = 713.5 Hz, PF_6).

Complex Ru$_5$: The complex **Ru$_5$** was prepared in the same manner as our published procedure using ligand **C$_5$** (1.00 g, 2.80 mmol), $[RuCl_2$(*p*-cymene)]$_2$ (1.72 g, 2.80 mmol) and NH_4PF_6 (0.92 g, 5.60 mmol). Yield: 2.03 g (61%). Yellow powder. m.p.: 243–245 ^{0}C. Elemental analysis: calcd (%) for $C_{42}H_{64}Cl_2F_{12}N_4P_2Ru_2$ (MW: 1187,96): C, 42.46; H, 5.43; N, 4.72%. Found: C, 42.44; H, 5.45; N, 4.73%. ^{1}H NMR (400 MHz, DMSO): δ 8.80 (d, J = 8.0 Hz, 2H, Ar-*H*), 7.80 (m, 2H, Ar-*H*), 6.93 (br, 1H, N*H*), 6.70 (br, 1H, N*H*), 5.45 (d, J = 5.6 Hz, 2H, *p*-cymene-*H*), 5.11 (d, J = 5.6 Hz, 2H, *p*-cymene-*H*), 4.52 (d, J = 5.6 Hz, 2H, *p*-cymene-*H*), 3.98 (d, J = 5.6 Hz, 2H, *p*-cymene-*H*), 3.00 (m, 6H,

NCH_2CH_2N and Bu-CH_2), 2.52 (m, 1H, *p*-cymene-C*H*), 1.92 (s, 3H, *p*-cymene-CH_3), 1.71 (m, 2H, Bu-CH_2), 1.36 (m, 2H, Bu-CH_2), 1.10 (d, J = 6.4 Hz, 3H, *p*-cymene-CH(CH_3)$_2$), 1.03 (d, J = 6.4 Hz, 3H, *p*-cymene-CH(CH_3)$_2$), 0.96 (t, J = 7.2 Hz, 3H, Bu-CH_3). ^{13}C NMR (100 MHz, DMSO): δ 146.8, 146.7, 126.5, 126.4, 125.9, 125.7, 122.3, 116.7, 116.3, 108.4, 107.8, 93.9, 93.3, 88.0, 87.2, 84.1, 83.8, 79.4, 78.7, 78.1, 77.4, 56.2, 56.2, 53.3, 52.9, 47.9, 47.8, 30.6, 30.5, 30.2, 22.7, 21.4, 21.2, 20.3, 17.0, 16.8, 14.2. ^{19}F NMR (376.2 MHz, DMSO): δ −69.2, −71.1 (d, $J_{F\text{-}F}$ = 711.3 Hz, PF_6). ^{31}P NMR (161.8 MHz, DMSO): δ −144.2 (septed, $J_{P\text{-}P}$ = 714.0 Hz, PF_6).

Complex Ru$_6$: The complex **Ru$_6$** was prepared in the same manner as our published procedure using ligand **C$_6$** (1.00 g, 3.26 mmol,), [RuCl$_2$(*p*-cymene)]$_2$ (1.99 g, 3.26 mmol) and NH_4PF_6 (1.06 g, 6.52 mmol). Yield: 2.30 g (62%). Yellow powder. m. p.: 237–239 °C. Elemental analysis: calcd (%) for $C_{38}H_{62}Cl_2F_{12}N_4P_2Ru_2$ (MW: 1137,90): C, 40.11; H, 5.49; N, 4.92%. Found: C, 40.13; H, 5.50; N, 4.90%. ^{1}H NMR (400 MHz, DMSO): δ 7.49 (s, 2H, Ar-*H*), 6.73 (br, 1H, N*H*), 6.41 (br, 1H, N*H*), 5.61 (d, J = 6.4 Hz, 2H, *p*-cymene-*H*), 5.40 (d, J = 6.0 Hz, 2H, *p*-cymene-*H*), 4.85 (d, J = 6.0 Hz, 2H, *p*-cymene-*H*), 4.72 (d, J = 6.0 Hz, 2H, *p*-cymene-*H*), 2.94 (m, 5H, NCH_2CH_2N and Bu-CH_2), 2.65 (m, 1H, *p*-cymene-C*H*), 2.14 (s, 3H, *p*-cymene-CH_3), 2.00 (m, 1H, Bu-CH_2), 1.66 (m, 2H, Bu-CH_2), 1.35 (m, 2H, Bu-CH_2), 1.19 (d, J = 6.8 Hz, 3H, *p*-cymene-CH(CH_3)$_2$), 1.13 (d, J = 6.8 Hz, 3H, *p*-cymene-CH(CH_3)$_2$), 0.94 (t, J = 7.2 Hz, 3H, Bu-CH_3). ^{13}C NMR (100 MHz, DMSO): δ 147.9, 106.7, 94.6, 85.8, 83.2, 80.8, 80.0, 56.3, 53.0, 48.6, 30.5, 30.3, 22.7, 21.6, 20.2, 17.3, 14.2. ^{19}F NMR (376.2 MHz, DMSO): δ −69.2, −71.1 (d, $J_{F\text{-}F}$ = 711.0 Hz, PF_6). ^{31}P NMR (161.8 MHz, DMSO): δ −144.1 (septed, $J_{P\text{-}P}$ = 713.8 Hz, PF_6).

4.6. CV experiments

The three electrode system consisted of a platinum disk as the working electrode, platinum wire as the counter electrode and saturated Ag/AgCl as the reference electrodes. The voltommograms were recorded at DMSO in the presence of 0.1 M of tetrabutylammonium hexaflouroborate solution. Potential scan was performed between −2.5 and +2.0 V.

4.7. Cell culture

Human cell lines such as cervix adenocarcinoma HeLa, androgen-dependent lymph node metastasis prostate adenocarcinoma LNCaP, androgen-independent bone metastasis prostate adenocarcinoma PC-3, androgen-independent brain metastasis prostate adenocarcinoma DU145, estrogen-responsive primary breast adenocarcinoma MCF-7, estrogen-unresponsive metastatic breast adenocarcinoma cell line MDA-MB-231, liver hepatocellular carcinoma HepG2, colorectal adenocarcinoma HT-29, bone osteosarcoma Saos-2 as well as normal fibroblast 3T3-L1 and Vero (African green monkey kidney) were purchased from ATCC (American type culture collection). LNCaP, MCF-7, MDA-MB-231, Saos-2 and HepG2 cell lines were maintained in RPMI-1640 while PC-3, DU145, HeLa, 3T3 and Vero cell lines were maintained in DMEM-F12 supplemented with 10% FBS (Fetal bovine Serum) (Invitrogen, UK), 1% L–glutamine (Invitrogen, UK), and 1% penicillin–streptomycin (Invitrogen, UK) in a humidified incubator at 37 °C and 5% CO_2. The morphology of the cells was examined every second day using a phase-contrast inverted microscope (CK40-F200; Olympus, Tokyo, Japan) and photographed. When the cells were confluent, they were routinely sub-cultured using 0.25% trypsin–ethylenediaminetetraacetic acid (EDTA) solution.

4.8. DNA binding

DNA binding experiments of **Ru$_3$** and **Ru$_6$** complexes were performed in the Tris-HCl buffer (20 mM Tris-HCl/NaCl, pH 0 7.0) with 0.1 mM FS-DNA using UV spectroscopy in order to investigate the possible binding modes to FS-DNA and to calculate the binding constants (Kb). The intrinsic binding constants (Kb) were calculated according to the Benesi-Hildebrand equation HYPERLINK "SPS:refid::bib52" [51].

$$1/(A - A_0) = 1/\{K_b(A_{max} - A_0)[Q]\} + 1/[A_{max} - A_0]$$

where A_0 is the absorption intensity of DNA at 260 nm in the absence of complex, A_{max} is the saturated absorption intensity of the DNA-metal complex adduct, A is the absorption intensity of DNA interacted with a metal complex and [Q] is the concentration of the metal complex. The binding constant (K_b) was graphically evaluated by plotting $1/[A - A_0]$ versus $1/[Q]$.

4.9. Application of Ru complexes

A stock solution of Ru complexes was prepared at a concentration of 10 mM in the cell culture medium. The stock solution was diluted 1/2, 1/4, 1/8, 1/16 and 1/32 with the medium solution. Then, 100 µL of cancer cell was added to each well from all dilutions prepared, including stock solution, and cells were incubated for 48 h in 37 °C and 5% CO_2.

4.10. Cell viability analyses with MTT assay

The cell viability and proliferation rate were analyzed the tetrazolium reduction assayin all cells. The stock solution of 3-(4,5-dimethylthiazol-2-yl)-2,5-diphenyltetrazoliumbromide (MTT) was prepared in PBS (final concentration was 5000 mg/mL) and stored in 4 + ^{0}C. All types of cells were cultured in 96-well plates for 24 h and the density of cells in each well was 104 in 200 µL of culture medium. The culture medium from all wells was discarded and 200 µL per well of 1/10 diluted MTT solution was added and then incubated for 3 h at 37 ^{0}C after incubation. 200 µL of MTT solvent (DMSO) was added to each well and it was then shaken on an orbital shaker for 15 min. Absorbance was measured at 570 nm with a 690 nm reference filter [48,49].

Acknowledgements

The authors thank Ege University (Project Number: 17-FEN-042) and the Scientific and Technological Research Council of Turkey (TUBITAK, Project Number: 214Z098) for their financial support. The authors acknowledge the Scientific and Technological Research Application and Research Center, Sinop University, Turkey, for the use of the Bruker D8 QUEST diffractometer.

Declaration of Competing Interest

The authors declared that there is no conflict of interest.

Appendix A. Supplementary material

Supplementary data to this article can be found online at https://doi.org/10.1016/j.bioorg.2020.103793.

References

[1] B. Rosenberg, L. VanCamp, J.E. Trosko, V.H. Mansour, Platinum compounds: a new class of potent antitumour agents, Nature 222 (1969) 385–386.
[2] Y.K. Yan, M. Melchart, A. Habtemariam, P.J. Sadler, Organometallic chemistry, biology and medicine: ruthenium arene anticancer complexes, Chem. Commun. (2005) 4764–4776.
[3] D. Wang, Stephen J. Lippard, Cellular processing of platinum anticancer drugs, Nat. Rev. Drug Discov. 4 (2005) 307–320.
[4] B. Tylkowski, R. Jastrząb, A. Odani, Developments in platinum anticancer drugs, Phys. Sci. Rev. 3 (2016) 1.
[5] B. Wong, L. Vancamp, J.E. Trosko, V.H. Mansour, Platinum Compounds: a new class of potent antitumour agents, Nature 222 (1969) 385–386.
[6] J. Reedijk, Improved understanding in platinium antitumour chemistry, Chem. Commun. (1996) 801–806.
[7] S.H. van Rijt, P.J. Sadler, Current applications and future potential for bioinorganic

chemistry in the development of anticancer drugs, Drug Discov. Today 14 (2009) 1089–1097.
[8] Z. Guo, P.J. Sadler, Metals in medicine, Angew. Chem. Int. Ed. 38 (1999) 1512–1531.
[9] J. Reedijk, Platinum Anticancer Coordination Compounds: Study of DNA binding inspires new drug design, Eur. J. Inorg. Chem. 10 (2009) 1303–1312.
[10] E. Wong, C.M. Giandomenico, Current status of platinum-based antitumor drugs, Chem. Rev. 99 (1999) 2451–2465.
[11] C. Scolaro, A. Bergamo, L. Brescacin, R. Delfino, M. Cocchietto, G. Laurenczy, T.J. Geldbach, G. Sava, P.J. Dyson, *In vitro* and *in vivo* evaluation of ruthenium(II)-arene PTA complexes, J. Med. Chem. 48 (2005) 4161–4171.
[12] H.M. Pineto, J.H. Schornagel (Eds.), Platinum and Other Metal Coordination Compounds in Cancer Chemotherapy, Plenum, New York, 1996.
[13] B. Therrien, W. Ang, F. Chérioux, L. Vieille-Petit, L. Juillerat-Jeanneret, G. Süss-Fink, P. Dyson, J. Cluster Sci. 18 (2007) 741–752.
[14] C.S. Allardayce, P.J. Dyson, Ruthenium in medicine: Current clinical uses and future prospects, Platinum Met. Rev. 45 (2001) 62–69.
[15] I. Romero-Canelón, L. Salassa, P.J. Sadler, The contrasting activity of iodido versus chlorido ruthenium and osmium arene azo- and imino-pyridine anticancer complexes: control of cell selectivity, cross-resistance, p53 dependence, and apoptosis pathway, J. Med. Chem. 56 (2013) 1291–1300.
[16] I.N. Stepanenko, A. Casini, F. Edafe, M.S. Novak, V.B. Arion, P.J. Dyson, M.A. Jakupec, B.K. Keppler, Conjugation of organoruthenium(II) 3-(1H-benzimidazol-2-yl)pyrazolo[3,4-b]pyridines and indolo[3,2-d]benzazepines to recombinant human serum albumin: a strategy to enhance cytotoxicity in cancer cells, Inorg. Chem. 50 (2011) 12669–12679.
[17] A.R. Timerbaev, C.G. Hartinger, S.S. Aleksenko, B.K. Keppler, Interactions of antitumor metallodrugs with serum proteins: advances in characterization using modern analytical methodology, Chem. Rev. 106 (2006) 2224–2248.
[18] A.Y. Shmykov, V.N. Filippov, L.S. Foteeva, B.K. Keppler, A.R. Timerbaev, Toward high-throughput monitoring of metallodrug-protein interaction using capillary electrophoresis in chemically modified capillaries, Anal. Biochem. 379 (2008) 216–218.
[19] M. Groessl, M. Terenghi, A. Casini, L. Elviri, R. Lobinski, P.J. Dyson, Reactivity of anticancer metallodrugs with serum proteins: new insights from size exclusion chromatography-ICP-MS and ESI-MS, J. Anal. At. Spectrom. 25 (2010) 305–313.
[20] I. Ascone, L. Messori, A. Casini, C. Gabbiani, A. Balerna, F. Dell'Unto, A.C. Castellano, Exploiting soft and hard X-ray absorption spectroscopy to characterize metallodrug/protein interactions: the binding of [trans-$RuCl_4$(Im)(dimethylsulfoxide)][ImH] (Im = imidazole) to bovine serum albumin, Inorg. Chem. 47 (2008) 8629–8634.
[21] S. Thangavel, R. Rajamanikandan, H.B. Friedrich, M. Ilanchelian, B. Omondi, Binding interaction, conformational change, and molecular docking study of N-(pyridin-2-ylmethylene)aniline derivatives and carbazole Ru(II) complexes with human serum albumins, Polyhedron 107 (2016) 124–135.
[22] M.J. Clarke, Oncological implication of the chemistry of ruthenium, Met. Ions Biol. Syst. 11 (1980) 231–283.
[23] A. Bergamo, C. Gaiddon, J.H.M. Schellens, J.H. Beijnen, G. Sava, Approaching tumour therapy beyond platinum drugs: status of the art and perspectives of ruthenium drug candidates, J. Inorg. Biochem. 106 (2012) 90–99.
[24] J.M. Rademaker-Lakhai, D. van den Bongard, D. Pluim, J.H. Beijnen, J.H.M. Schellens, A Phase I and pharmacological study with imidazolium-trans-DMSO-imidazole-tetrachlororuthenate, a novel ruthenium anticancer agent, Clin. Cancer Res. 10 (2004) 3717–3727.
[25] S. Leijen, S.A. Burgers, P. Baas, D. Pluim, M. Tibben, E. van Werkhoven, E. Alessio, G. Sava, J.H. Beijnen, J.H.M. Schellens, Phase I/II study with ruthenium compound NAMI-A and gemcitabine in patients with non-small cell lung cancer after first line therapy, Invest. New Drugs 33 (2015) 201–214.
[26] C.G. Hartinger, S. Zorbas-Seifried, M.A. Jakupec, B. Kynast, H. Zorbas, B.K. Keppler, From bench to bedside–preclinical and early clinical development of the anticancer agent indazolium trans-[tetrachlorobis(1H-indazole)ruthenate(III)] (KP1019 or FFC14A), J. Inorg. Biochem. 100 (2006) 891–904.
[27] M. Clarke, Ruthenium metallopharmaceuticals, J. Coord. Chem. Rev. 236 (2003) 209–233.
[28] R.E. Morris, R.E. Aird, P.D. Murdoch, H.M. Chen, J. Cummings, N.D. Hughes, S. Parsons, A. Parkin, G. Boyd, D.I. Jodrell, P.J. Sadler, Inhibition of cancer cell growth by ruthenium(II) arene complexes, J. Med. Chem. 44 (2001) 3616–3621.
[29] W. Han Ang, P.J. Dyson, Classical and Non-classical ruthenium-based anticancer drugs: towards targeted chemotherapy, Eur. J. Inorg. Chem. 2006 (2006) 4003–4018.
[30] S.J. Dougan, M. Melchart, A. Habtemariam, S. Parsons, P.J. Sadler, Phenylazopyridine and phenylazo-pyrazole chlorido ruthenium(II) arene complexes: arene loss, aquation, and cancer cell cytotoxicity, Inorg. Chem. 45 (2006) 10882–10894.
[31] A. Habtemariam, M. Melchart, R. Fernández, S. Parsons, Iain D. H. Oswald, A. Parkin, F.P.A. Fabbiani, J.E. Davidson, A. Dawson, R.E. Aird, D.I. Jodrell, P.J. Sadler, Structure-activity relationships for cytotoxic ruthenium(II) arene complexes containing N,N-, N,O-, and O,O-chelating ligands, J. Med. Chem. 49 (2006) 6858–6868.
[32] T. Bugarcic, A. Habtemariam, R.J. Deeth, F.P.A. Fabbiani, S. Parsons, P.J. Sadler, Ruthenium(II) arene anticancer complexes with redox-active diamine ligands, Inorg. Chem. 48 (2009) 9444–9453.
[33] Serdar Batıkan Kavukcu, Salih Günnaz, Onur Şahin, Hayati Türkmen, Piano-stool Ru (II) arene complexes that contain ethylenediamine and application in alpha-alkylation reaction of ketones with alcohols, Appl Organometal Chem 33 (5) (2019) e4888 https://onlinelibrary.wiley.com/toc/10990739/33/5 https://onlinelibrary.wiley.com/doi/abs/10.1002/aoc.4888https://doi.org/10.1002/aoc.v33.510.1002/aoc.4888.
[34] J.X. Ong, C.W. Yap, W.H. Ang, Rational design of selective organoruthenium inhibitors of protein tyrosine phosphatase 1B, Inorg. Chem. 51 (2012) 12483–12492.
[35] S. Grgurić-Šipka, I. Ivanović, G. Rakić, N. Todorović, N. Gligorijević, S. Radulović, V.B. Arion, B.K. Keppler, Ž.L. Tešić, Ruthenium(II)-arene complexes with functionalized pyridines: synthesis, characterization and cytotoxic activity, Eur. J. Med. Chem. 45 (2010) 1051–1058.
[36] M.G. Mendoza-Ferri, C.G. Hartinger, R.E. Eichinger, N. Stolyarova, K. Severin, M.A. Jakupec, A.A. Nazarov, B.K. Keppler, Influence of the spacer length on the in Vitro anticancer activity of dinuclear ruthenium − arene compounds organometallics 27 (2008) 2405–2407.
[37] M.G. Mendoza-Ferri, C.G. Hartinger, M.A. Mendoza, M. Groessl, A.E. Egger, R.E. Eichinger, J.B. Mangrum, N.P. Farrell, M. Maruszak, P.J. Bednarski, F. Klein, M.A. Jakupec, A.A. Nazarov, K. Severin, B.K. Keppler, Transferring the concept of multinuclearity to ruthenium complexes for improvement of anticancer activity, J. Med. Chem. 52 (2009) 916–925.
[38] O. Novakova, A.A. Nazarov, C.G. Hartinger, B.K. Keppler, V. Brabec, DNA interactions of dinuclear RuII arene antitumor complexes in cell-free media, Biochem. Pharmacol. 77 (2009) 364–374.
[39] H. Chen, J.A. Parkinson, O. Nováková, J. Bella, F. Wang, A. Dawson, R. Gould, S. Parsons, V. Brabec, P.J. Sadler, Induced-fit recognition of DNA by organometallic complexes with dynamic stereogenic centers, PNAS 100 (2003) 14623–14628.
[40] J. Zhao, S. Li, X. Wang, G. Xu, S. Gou, Dinuclear organoruthenium complexes exhibiting antiproliferative activity through DNA damage and a reactive-oxygen-species-mediated endoplasmic reticulum stress pathway, Inorg. Chem. 58 (2019) 2208–2217.
[41] R.E. Aird, J. Cummings, A.A. Ritchie, M. Muir, R.E. Morris, H. Chen, P.J. Sadler, D.I. Jodrell, *In vitro* and *in vivo* activity and cross resistance profiles of novel ruthenium (II) organometallic arene complexes in human ovarian cancer, Br. J. Cancer 86 (2002) 1652–1657.
[42] F. Linares, M.A. Galindo, S. Galli, M.A. Romero, J.A. Navarro, E. Barea, Tetranuclear coordination assemblies based on half-sandwich ruthenium(II) complexes: noncovalent binding to DNA and cytotoxicity, Inorg. Chem. 48 (2009) 7413–7420.
[43] L. Zeng, P. Gupta, Y. Chen, E. Wang, L. Ji, H. Chao, Zhe-Sheng Chen, The development of anticancer ruthenium(II) complexes: from single molecule compounds to nanomaterials, Chem. Soc. Rev. 46 (2017) 5771–5804.
[44] O. Nováková, A.A. Nazarov, C.G. Hartinger, B.K. Keppler, V. Brabec, DNA interactions of dinuclear RuII arene antitumor complexes in cell-free media, Biochem. Pharmacol. 77 (2009) 364–374.
[45] L.K. Batchelor, P.J. Dyson, Extrapolating the fragment-based approach to inorganic drug discovery, Trends Chem. 1 (2019) 7.
[46] L. Gök, S. Günnaz, Z.S. Şahin, L. Pelit, H. Türkmen, The imidazo{[4,5-f][1,10]-phenanthrolin}l-2-ylidene and its palladium complexes: Synthesis, characterization, and application in C-C cross-coupling reactions, J. Organomet. Chem. 827 (2017) 96–104.
[47] M.A. Bennett, A.K. Smith, Arene ruthenium(II) complexes formed by dehydrogenation of cyclohexadienes with ruthenium(III) trichloride, J. Chem. Soc. Dalton Trans. (1974) 233–241.
[48] O. Kurt, F. Ozdal-Kurt, M.I. Tuğlu, C.M. Akçora, The cytotoxic, neurotoxic, apoptotic and antiproliferative activities of extracts of some marine algae on the MCF-7 cell line, Biotech Histochem. 89 (2014) 568–576.
[49] H. Seda Vatansever, K. Sorkun, S. Ismet Deliloğlu Gurhan, F. Ozdal-Kurt, E. Turkoz, O. Gencay, B. Salih, Propolis from Turkey induces apoptosis through activating caspases in human breast carcinoma cell lines, Acta Histochem. 112 (2010) 546–556.
[50] V.T. Yilmaz, C. Icsel, O.R. Turgut, M. Aygun, M. Erkisa, M.H. Turkdemir, E. Ulukaya, Synthesis, structures and anticancer potentials of platinum(II) saccharinate complexes of tertiary phosphines with phenyl and cyclohexyl groups targeting mitochondria and DNA, Eur. J. Med. Chem. 155 (2018) 609–622.
[51] H.A. Benesi, J.H.A. Hidebrand, Spectrophotometric investigation of the interaction of iodine with aromatic hydrocarbons, J. Am. Chem. Soc. 71 (1949) 2703–2707.